Articles

Dodecamer DNA Duplex Formation Is Characterized by Second-Order Kinetics, Positive Activation Energies, and a Dependence on Sequence and Mg^{2+} Ion Concentration†

Ernesto Carrillo-Nava, Yamilet Mejía-Radillo, and Hans-Jürgen Hinz*

Institut für Physikalische Chemie der Westfälischen Wilhelms-Universität Münster, Corrensstrasse 30, 48149 Münster, Germany, and Center for Nanotechnology (CeNTech), Heisenbergstrasse 11, 48149 Münster, Germany

Received September 25, 2008; Revised Manuscript Received October 29, 2008

ABSTRACT: This study provides quantitative information about the kinetics of formation of a complex between DNA oligomers having 12 bp. The DNA dodecamers were designed in such a way as to avoid the formation of hairpins or slipped duplex structures within single strands. The hybridization was carried out employing stopped-flow techniques. The reaction was studied in different buffers (phosphate or cacodylate), in the presence and absence of Mg^{2+} ions, and at different temperatures. Under all conditions, the reaction followed second-order kinetics. The association rate constants were on the order of 10^6 M^{-1} s^{-1} and were found to increase with an increase in temperature. Both the rate constants and the positive activation energies of the two dodecamers, which differ only by the presence of the TAGG tetrad either at the 3′ end or at the 5′ end, turned out to be significantly different. The presence of Mg^{2+} ions had a profound influence on the kinetics of association of either compound by substantially decreasing the activation energy of the process. The dependence on sequence of the kinetics of hybridization was manifest in all parameters under all the experimental conditions.

Over the past five decades, there has been continuous research on the kinetic and thermodynamic characterization of the various structures that can be formed between cDNA and RNA or DNA sequences. These studies were primarily driven by the fundamental interest in quantifying the dynamics and energetics of processing genetic information and by the attempts to understand the nature of the intra- and intermolecular forces associated with the mechanism of the helix−coil transition of oligo- and polynucleotides (*1*−*4*). Today there is a renewed interest in the specific and programmable oligonucleotide interactions mainly due to their promising applications in DNA-based nanotechnology such as DNA chip technology or functionalized nanoparticles (*5*−*14*). Despite the great analytical and medical potential of DNA oligonucleotides, relatively few studies have been concerned with the quantitative kinetic and thermodynamic aspects of duplex formation, although the availability of rate constants and equilibrium parameters is fundamentally important for the successful design of analytical or biomedical applications such as polymerase chain reaction (PCR), RCA, and in situ hybridization (*15*).

In this study, we report rate constants of duplex formation of two pairs of cDNA oligonucleotide 12-mers in two buffer systems, as a function of temperature and Mg^{2+} ion concentration and depending on sequence variations with a constant GC:AT ratio. In following this strategy, we intend to provide a reference system of free oligonucleotides to which functionalized DNA systems can be compared.

MATERIALS AND METHODS

Oligonucleotide Preparation and Characterization. The sequences of the oligonucleotides studied together with their molar absorption coefficients, ε, are shown in the following scheme:

Sequence	name	ε [M^{-1} cm^{-1}]
5'-**TAG G**TC AAT ACT-3'	Strand **Ia**	120600
3'-**ATC C**AG TTA TGA-5'	Strand **Ib**	123200
5'-**ATC C**TC AAT ACT-3'	Strand **IIa**	114300
3'-**TAG G**AG TTA TGA-5'	Strand **IIb**	128500

The 12-mers differ in that the four bases marked in bold occur either at the 3′ end or at the 5′ end. The residual eight bases are identical. It should be emphasized that none of the single strands can form hairpins or can hybridize with the complementary strand out of register.

† This work was supported by a research grant from BMBF to H.-J.H.

* To whom correspondence should be addressed. Phone: +49 251 53406 855. E-mail: hinz@uni-muenster.de.

10.1021/bi801821m CCC: $40.75
Published on Web 11/17/2008

Table 1: Observed Second-Order Rate Constants for the Hybridization of 12-mers **Ia** and **Ib** in Two Buffers and in the Presence of 10 mM $MgCl_2$

	k_{obs} ($\times 10^{-6}$ M^{-1} s^{-1})		
temp (°C)	10 mM $MgCl_2$, 10 mM $(CH_3)_2AsONa$, 100 mM NaCl, pH 7.0	10 mM $(CH_3)_2AsONa$, 100 mM NaCl, pH 7.0	10 mM NaH_2PO_4, 100 mM NaCl, pH 7.0
10	–	0.168 ± 0.00018	0.241 ± 0.002
15	1.832 ± 0.0023	0.296 ± 0.0025	0.475 ± 0.004
20	2.500 ± 0.0053	0.300 ± 0.0029	0.562 ± 0.004
25	2.996 ± 0.0041	0.518 ± 0.0051	0.705 ± 0.004
30	4.043 ± 0.0109	0.654 ± 0.0067	0.869 ± 0.0010
35	5.314 ± 0.0120	0.785 ± 0.0083	1.229 ± 0.0011
40	5.38 ± 0.0101	–	–

The oligonucleotides were synthesized using standard phosphoramidite chemistry. They were purified via high-performance liquid chromatography (HPLC) and lyophilized in a centrifuge under vacuum. The purity and composition of each oligonucleotide were verified by mass spectrometry using the matrix-assisted laser desorption ionization (MALDI) method. DNA concentrations were determined spectrophotometrically by measuring the absorbance at 260 nm and using the corresponding extinction coefficients given in Table 1, which were calculated using the nearest neighbor approximation (*16*).

Stopped-Flow Experiments. With the exception of one experiment, where we employed single-strand concentrations of 2 μM, routinely equal amounts of the complementary single strands of 4 μM each were mixed for hybridization. Three buffer systems were used to check the influence of the buffer material itself and to evaluate the influence of Mg^{2+} ions: (a) phosphate buffer (10 mM NaH_2PO_4, 100 mM NaCl, pH 7.0), (b) cacodylate buffer with $MgCl_2$ (10 mM $MgCl_2$, 10 mM $(CH_3)_2AsONa$, 100 mM NaCl, pH 7.0), and (c) cacodylate buffer without $MgCl_2$ (10 mM $(CH_3)_2AsONa$, 100 mM NaCl, pH 7.0).

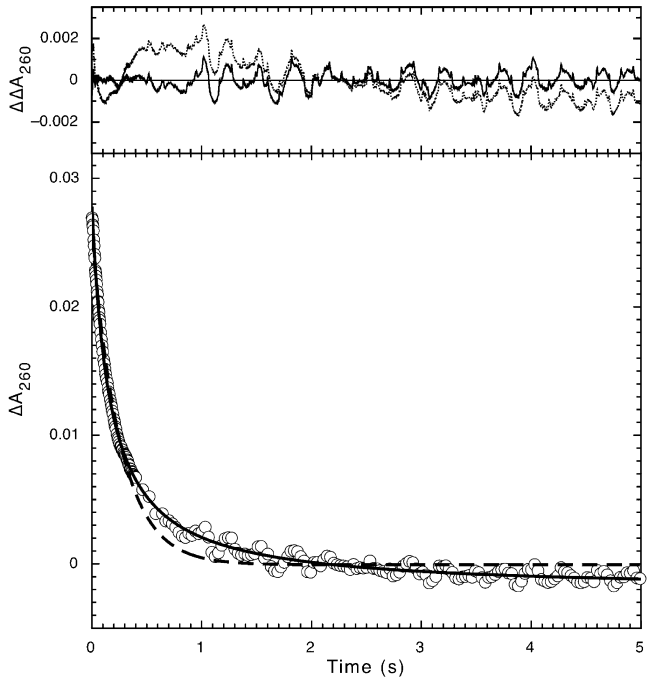

FIGURE 1: Typical time course of the absorbance change at 260 nm associated with duplex formation. The graph shows hybridization of single-stranded dodecamers **IIa** and **IIb** at 30 °C in phosphate buffer (10 mM NaH_2PO_4, 100 mM NaCl, pH 7.0). Oligonucleotide concentrations were 4 μM each. The circles represent the averaged experimental data obtained from 10 individual experiments. The solid line represents the fit assuming second-order kinetics, and the dashed line shows the fit assuming first-order kinetics. In all experiments, hybridization exhibited second-order kinetics. The top part shows the deviations between the fit curves for first- or second-order fits and experimental values.

The stopped-flow measurements were performed using the SFM-400 stopped-flow module from Bio-Logic SAS (Grenoble, France) coupled with the MOS-200 optical system (Bio-Logic SAS) which uses a Xe arc light source attached to a manual monochromator on an optical bench. The temperature of the stopped-flow SFM-400 unit was controlled to a precision of 0.05 °C by a Thermo Haake (Paramus, NJ) F6/C25 water bath. Measurements were performed at 10, 15, 20, 25, 30, 35, and 40 °C. After equal volumes of the complementary oligonucleotides had been rapidly mixed, the decrease in absorbance at 260 nm was recorded as a function of time. Up to 6500 pairs of absorbance−time data points were accumulated in each experiment. Data sets of 10 experiments performed under identical conditions were averaged and fitted to a first- and second-order reaction scheme using Bio-Kine 32 version 4.40 provided by Bio-Logic SAS.

RESULTS

Kinetics of Double Helix Formation of 12-mers. The association process between two complementary short chain oligonucleotides to form a double helix can be represented by the equation

$$ss_1 + ss_2 \rightarrow ds \quad (1)$$

where ss_1 and ss_2 represent complementary single strands 1 and 2, respectively, and ds is the double helix. In previous studies on oligoribouridylic−oligoriboadenylic nucleotides, the reaction has been found to follow a second-order rate law (*2*)

$$\frac{d[ds]}{dt} = -\frac{d[ss_1]}{dt} = k_{obs}[ss_1][ss_2] \quad (2)$$

As the present experiments were designed in such a way that the concentration of the complementary single strands was always identical, the rate law assumes the simple form

$$-\frac{d[ss_1]}{dt} = k_{obs}[ss_1]^2 \quad (3)$$

This rate law or rather its integrated form was the basis for the evaluation of the experimental data.

A typical stopped-flow experiment of the recombination of complementary dodecamers **IIa** and **IIb** is shown in Figure 1 together with curves of second-order (solid line) and first-

Table 2: Observed Second-Order Rate Constants for the Hybridization of 12-mers **IIa** and **IIb** in Two Buffers and in the Presence of 10 mM $MgCl_2$

	k_{obs} ($\times 10^{-6}$ M^{-1} s^{-1})		
temp (°C)	10 mM $MgCl_2$, 10 mM $(CH_3)_2AsONa$, 100 mM NaCl, pH 7.0	10 mM $(CH_3)_2AsONa$, 100 mM NaCl, pH 7.0	10 mM NaH_2PO_4, 100 mM NaCl, pH 7.0
10	3.811 ± 0.0018	0.804 ± 0.0011	1.092 ± 0.0013
15	4.482 ± 0.0045	1.076 ± 0.0030	1.340 ± 0.0009
20	4.819 ± 0.0027	1.286 ± 0.0015	1.591 ± 0.0010
25	5.572 ± 0.0034	1.332 ± 0.0010	1.864 ± 0.0012
30	6.569 ± 0.0089	1.598 ± 0.0014	1.951 ± 0.0018
35	7.191 ± 0.0095	1.783 ± 0.0017	2.269 ± 0.0022
40	8.134 ± 0.0093	–	–

order (dashed curve) fits. The experimental trace shown in the figure is the average of 10 independent measurements. It is evident that only the second-order fit represents the kinetic trace properly, in agreement with our assumption and previous *T*-jump relaxation and stopped-flow studies (*2, 17*). The second order in concentration was verified under all experimental conditions applied in this study. Generally, the deviations between experimental and fit curves were substantially smaller for second-order fits compared to first-order fits, as shown in the top part of Figure 1. The corresponding χ^2 values for second-order fits were usually smaller by a factor of 10. Tables 1 and 2 summarize the values of the second-order rate constants (k_{obs}) observed for the hybridization between the complementary oligonucleotide sequences of 12-mers **Ia** and **Ib** and 12-mers **IIa** and **IIb**, respectively. Measurements were taken at six or seven temperatures and in three different buffer systems.

Several noteworthy features become obvious on inspection of the data. (a) The rate constants of hybridization are similar in order of magnitude for all systems. (b) Under all conditions, the rate constants are dependent on temperature, and they increase with an increase in temperature. (c) The presence of Mg^{2+} ions accelerates the hybridization process significantly, as the increased rate constants demonstrate. (d) The small difference in primary structure between sequences **I** and **II** has a significant effect on the rate of hybridization, as the comparison between Tables 1 and 2 shows.

It is of great diagnostic value to know the activation energy of the hybridization reaction, as it permits us to infer a reaction mechanism or, at least, to exclude certain types of mechanisms.

Figure 2 shows the Arrhenius plots of the association rate constants determined under different experimental conditions. It is evident that all plots are linear which suggests that hybridization of all systems under the buffer conditions studied here is dominated by a single rate-limiting step. The activation energies, E_a, have been evaluated from the slope according to the Arrhenius relationship

$$\ln k_{obs} = -\frac{E_a}{RT} + \ln A \qquad (4)$$

It is highly remarkable that all plots of ln k_{obs} versus $1/T$ exhibit negative slopes, which are indicative of positive activation energies. The values of the activation energies are listed in Table 3. It is important to note that Mg^{2+} ions have a significant influence on the kinetics of hybridization. In the presence of Mg^{2+}, the activation energy is lower for both pairs of complementary oligonucleotides (**Ia** and **Ib**, and **IIa** and **IIb**), while the values of E_a are the same within experimental error for the two Mg-free buffers.

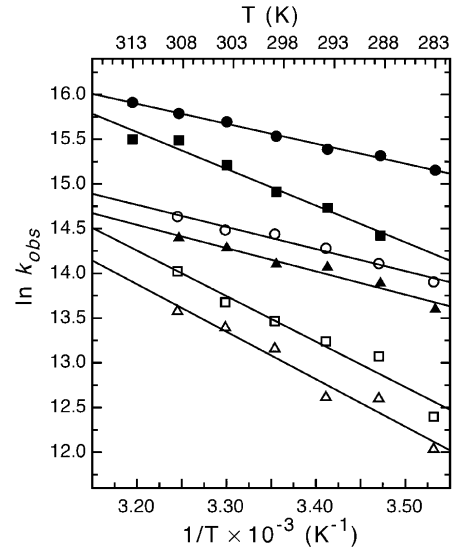

FIGURE 2: Arrhenius plots of the association rate constants of the DNA dodecamers observed by stopped-flow measurements. The different symbols represent the following experimental conditions: (●) **IIa** and **IIb** in 10 mM $MgCl_2$, 10 mM $(CH_3)_2AsONa$, and 100 mM NaCl at pH 7.0; (■) **Ia** and **Ib** in 10 mM $MgCl_2$, 10 mM $(CH_3)_2AsONa$, and 100 mM NaCl at pH 7.0; (○) **IIa** and **IIb** in 10 mM NaH_2PO_4 and 100 mM NaCl at pH 7.0; (□) **Ia** and **Ib** in 10 mM NaH_2PO_4 and 100 mM NaCl at pH 7.0; (▲) **IIa** and **IIb** in 10 mM $(CH_3)_2AsONa$ and 100 mM NaCl at pH 7.0; and (△) **Ia** and **Ib** in 10 mM $(CH_3)_2AsONa$ and 100 mM NaCl at pH 7.0. The solid lines represent linear fits of the data to eq 4.

Table 3: Activation Energies, E_a, of Formation of a Duplex between 12-mers **Ia** and **Ib** and 12-mers **IIa** and **IIb**, Derived from Second-Order Rate Constants

buffer	E_a (kJ/mol of oligomer) of **Ia** and **Ib**	E_a (kJ/mol of oligomer) of **IIa** and **IIb**
10 mM $MgCl_2$, 10 mM $(CH_3)_2AsONa$, 100 mM NaCl, pH 7.0	34.1 ± 2.8[a]	18.6 ± 0.6[b]
10 mM $(CH_3)_2AsONa$, 100 mM NaCl, pH 7.0	44.1 ± 4.5[b]	21.6 ± 2.3[b]
10 mM NaH_2PO_4, 100 mM NaCl, pH 7.0	42.3 ± 4.8[b]	20.5 ± 1.5[b]

[a] Final concentration of the duplex, 2.0 μM. [b] Final concentration of the duplex, 4.0 μM.

Inspection of the rate constants reveals another important result. The relatively small difference in primary structure between sequences **Ia** and **Ib** and sequences **IIa** and **IIb** has a significant effect on both the rate constants and the activation energy. Values of E_a are consistently smaller for formation of the **IIa**−**IIb** duplex than for formation of the **Ia**−**Ib** duplex in all buffers employed. We have no explanation for this finding.

DISCUSSION

The second-order rate constants for formation of a duplex of the two DNA 12-mers determined in this study by stopped-flow measurements are similar in magnitude as observed previously for the association of complementary oligonucleotides and poly(A+U) strands in an aqueous buffer solution. Literature values ranged from 4×10^5 to 2×10^7 M^{-1} s^{-1} (*2*−*4, 17*−*19*). The upper limit of the association rate constants can be considered as being characteristic of a diffusion-limited reaction. Similar rate constants were obtained also for formation of a duplex between DNA oligonucleotides and complementary locked nucleic acid (LNA) oligomers (*20, 21*) and oligonucleotides containing non-nucleotide inserts (*22*). It is particularly noteworthy that rate constants for DNA duplex formation at the single-molecule level within a protein nanopore were also found to be consistent with the values derived from macroscopic solution studies (*23*). An order of magnitude difference in the on-rate constant was observed when doubly dye-labeled 16-mers were employed (5.7×10^5 M^{-1} s^{-1}). The dyes were attached to render it possible to use Förster resonance energy transfer for monitoring double helix formation. The rate constant decreased by another factor of 10 when instead of the complementary oligomer the target sequence in phage M13mp18(+) was offered (*24*). While the rate constants for various oligonucleotides differing in length and GC content did not vary dramatically at 25 °C, the few studies involving different temperatures revealed significant differences in the temperature variation of the kinetic parameters. Arrhenius plots of the association rate constants resulted in activation energies for duplex formation that differed greatly in both sign and magnitude.

It has been argued that, from a kinetic standpoint, DNA duplex formation is not an elementary reaction but rather follows a reaction sequence, in which the rate-determining step is the formation of a nucleus that comprises a couple of base pairs. Once this nucleus has been created, the double helix can form very rapidly. Evidence for such a mechanism was derived from *T*-jump experiments using poly(A+U) duplexes on the basis of the observation of negative activation energies of approximately −38 kJ mol^{-1} (*2*). These negative activation energies were interpreted as being indicative of the formation of a nucleus consisting of three A-U base pairs before the residual double helix zips up fast. Very different kinetic behavior was subsequently determined by Pörschke et al. with oligonucleotides that contained, in addition to A and U, G or C (*4*). Helix formation of these oligonucleotides was exclusively characterized by positive activation parameters which showed a rather broad variation between approximately 12.5 and 54 kJ/mol, depending on sequence. The authors assigned this different behavior to the presence of two or three G-C base pairs in their oligonucleotides, of which two adjacent were considered enough for formation of a stable nucleation site. This interpretation is not supported by recent experiments of Gu et al. (*25*). These authors studied by *T*-jump measurements the recombination of two different DNA 10-mers: one having only two adjacent G-C pairs in the duplex and the other having a total of six G-C base pairs, of which two were adjacent. Thus, the duplexes differed significantly in temperature stability, although no transition temperatures or other stability parameters were reported. The association rate constants for duplex formation of the two sequences were 1.15×10^7 and 5.43×10^7 M^{-1} s^{-1}, respectively. What is, however, most interesting in this context is the finding of negative activation energies of approximately −18 kJ mol^{-1} for both duplexes, independent of the significant differences in their sequence. Furthermore, it was observed in this study that viscosity changes of the solution by addition of low- or high-mass PEGs[1] at 20 wt % did not significantly alter rate constants. Activation energies, however, increased from −18 kJ mol^{-1} for PEG 8000 to approximately −4 kJ mol^{-1} for PEG 200 but remained negative under all experimental conditions. These results are not consistent with those of Pörschke et al. (*4*) or with their interpretation that two adjacent G-C pairs would change the mechanism of association in such a manner that positive activation energies would result.

When we compare the results of this study with the literature data cited, there are differences and similarities. First, our single strands cannot form internal structures except for stacking, nor can they form duplexes out of register. Thus, there are no complications due to intermediate structures resulting from partial interactions such as those that occur in poly(A+U) or oligo-A and oligo-U systems. Second, the sequence variation does not involve shifts in the melting temperature, T_m, of the duplexes. This has an advantage in that the determination of rate constants at identical temperatures occurs for both duplexes always the same distance ($T_m - T$) from the melting temperature, a parameter which has been shown to be important for comparability of results by several authors (*1, 26, 27*). Third, we introduce a new aspect into the discussion of the influence of sequence differences on the kinetics of duplex formation. Our dodecamers differ only by the occurrence of the TAGG sequence at the 5′ or 3′ end of the oligomer. The residual 8 bp are identical. Nevertheless, we observed significant differences in the rate constants and in their variation with temperature. Duplex formation of sequences **Ia** and **Ib** showed consistently smaller rate constants at all temperatures. This conclusion holds for both cacodylate and phosphate buffer and also in the presence of 10 mM $MgCl_2$ in cacodylate buffer. There is a large difference in the activation energies of duplex formation between sequences **Ia** and **Ib** and sequences **IIa** and **IIb**. E_a is approximately 43 kJ mol^{-1} for the reaction between **Ia** and **Ib** in both buffers, whereas for formation of a duplex between **IIa** and **IIb**, it is only ∼21 kJ mol^{-1}. The presence of Mg^{2+} ions reduces the activation energy for both reactions. In the case of **Ia**−**Ib** hybridization, E_a is decreased to 34 kJ mol^{-1}; for formation of a complex between **IIa** and **IIb**, the activation energy is reduced to 18.5 kJ mol^{-1}.

The dramatic differences in activation parameters observed in this study for duplex formation between the rather similar DNA 12-mers are remarkable but so far escape molecular explanation. If it were only an ionic strength effect, it would be identical for the two reactions. As this is not the case, specific interactions with either the single strands or the double helices must be assumed to rationalize the increased number of productive encounters between one pair of complementary dodecamers. So far, we cannot identify the nature of these specific Mg^{2+} interactions. These results are

[1] Abbreviation: PEG, polyethylene glycol.

intriguing but show also that the level of understanding of seemingly simple hybridization reactions is far from being satisfactory.

ACKNOWLEDGMENT

We thank Mr. Nhat Tran and Prof. Dr. F. Seela (CeNTech) for the synthesis of the oligonucleotides and Dr. H. Luftmann for his characterization by MALDI spectrometry. We also thank Dr. B. Beerman for helpful discussions and Miss J. Guddorf for her excellent technical assistance.

REFERENCES

1. Wetmur, J. G., and Davidson, N. (1968) Kinetics of renaturation of DNA. *J. Mol. Biol. 31*, 349–370.
2. Pörschke, D., and Eigen, M. (1971) Co-operative non-enzymic base recognition. III. Kinetics of the helix-coil transition of the oligoribouridylic oligoriboadenylic acid system and of oligoriboadenylic acid alone at acidic pH. *J. Mol. Biol. 62*, 361–381.
3. Craig, M. E., Crothers, D. M., and Doty, P. (1971) Relaxation kinetics of dimer formation by self complementary oligonucleotides. *J. Mol. Biol. 62*, 383–401.
4. Pörschke, D., Uhlenbeck, O. C., and Martin, F. H. (1973) Thermodynamics and kinetics of the helix-coil transition of oligomers containing GC base pairs. *Biopolymers 12*, 1313–1335.
5. Mirkin, C. A., Letsinger, R. L., Mucic, R. C., and Storhoff, J. J. (1996) A DNA-based method for rationally assembling nanoparticles into macroscopic materials. *Nature 382*, 607–609.
6. Loweth, C. J., Caldwell, B. W., Peng, X., Alivisatos, A. P., and Schultz, P. G. (1999) DNA-based assembly of gold nanocrystals. *Angew. Chem., Int. Ed. 38*, 1808–1812.
7. Storhoff, J. J., and Mirkin, C. A. (1999) Programmed materials synthesis with DNA. *Chem. Rev. 99*, 1849–1862.
8. Niemeyer, C. M., and Mirkin, C. A. (2004) *NanoBiotechnology. Concepts, Methods, Applications*, Wiley-VCH, Weinheim, Germany.
9. Hazakira, P., Ceyhan, B., and Niemeyer, C. M. (2004) Reversible switching of DNA-gold nanoparticle aggregation. *Angew. Chem., Int. Ed. 43*, 6469–6471.
10. Park, S.-J., Lazarides, A. A., Storhoff, J. J., Pesce, L., and Mirkin, C. A. (2004) The structural characterization of oligonucleotide-modified gold nanoparticle networks formed by DNA hybridization. *J. Phys. Chem. B 108*, 12375–12380.
11. Dillenback, L. M., Goodrich, G. P., and Keating, C. D. (2006) Temperature-programmed assembly of DNA:Au nanoparticle bioconjugates. *Nano Lett. 6*, 16–23.
12. Hazarika, P., Kukolka, F., and Niemeyer, C. M. (2006) Reversible binding of fluorescent proteins at DNA-gold nanoparticles. *Angew. Chem., Int. Ed. 45*, 6827–6830.
13. Beermann, B., Carrillo-Nava, E., Scheffer, A., Buscher, W., Jawalekar, A. M., Seela, F., and Hinz, H.-J. (2007) Association temperature governs structure and apparent thermodynamics of DNA-gold nanoparticles. *Biophys. Chem. 126*, 124–131.
14. Lee, J.-S., Ulmann, P. A., Han, M. S., and Mirkin, C. A. (2008) A DNA-Gold Nanoparticle-Based Colorimetric Competition Assay for the Detection of Cysteine. *Nano Lett. 8*, 529–533.
15. Wu, P., Nakano, S., and Sugimoto, N. (2002) Temperature dependence of thermodynamic properties for DNA/DNA and RNA/DNA duplex formation. *Eur. J. Biochem. 269*, 2821–2830.
16. Cantor, C. R., Warshaw, M. M, and Shapiro, H. (1970) Oligonucleotide interactions. III. *Biopolymers 9*, 1059–1077.
17. Ross, P. D., and Sturtevant, J. M. (1962) On the kinetics and mechanics of helix formation: The two stranded poly (A + U) complex from polyriboadenylic acid and polyribouridylic acid. *J. Am. Chem. Soc. 84*, 4503–4507.
18. Riesner, D., and Römer, R. (1973) Thermodynamics and kinetics of conformational transitions in oligonucleotides and tRNA. In *Physico-chemical Properties of Nucleic Acids* (Duchesne, J., Ed.) pp 237−318, Academic Press, London.
19. Turner, D. H., Sugimoto, N., and Freier, S. M. (1990) Thermodynamics and kinetics of base-pairing and of DNA and RNA self-assembly and helix-coil transition. In *Landolt-Börnstein Numerical Data and Funcitional Relationships in Science and Technology. New Series, Group VII: Biophysics, Vol. 1 Nucleic Acids* (Madelung, O., Ed.) pp 218, Springer-Verlag, Berlin.
20. Christensen, U., Jacobsen, N., Rajwanshi, V. K., Wenger, J., and Koch, T. (2001) Stopped-flow kinetics of locked nucleic acid (LNA)-oligonucleotide duplex formation: Studies of LNA-DNA and DNA-DNA interactions. *Biochem. J. 354*, 481–484.
21. Christensen, U. (2007) Thermodynamic and kinetic characterization of duplex formation between 2′-O,4′-C-Methylene-modified oligoribonucleotides, DNA and RNA. *Biosci. Rep. 27*, 327–333.
22. Pyshnyi, D. V., Lomzov, A. A., Pyshnaya, I. A., and Ivanova, E. M. (2006) Hybridization of the bridged oligonucleotides with DNA: Thermodynamic and kinetic studies. *J. Biomol. Struct. Dyn. 23*, 567–579.
23. Howorka, S., Movileanu, L., Braha, O., and Bayley, H. (2001) Kinetics of duplex formation for individual DNA strands within a single protein nanopore. *Proc. Natl. Acad. Sci. U.S.A. 98*, 12996–13001.
24. Parkhurst, K. M., and Parkhurst, L. J. (1995) Kinetic studies by fluorescence resonance energy transfer employing a double-labeled oligonucleotide: Hybridzation to the oligonucleotide complement and to single-stranded DNA. *Biochemistry 34*, 285–292.
25. Gu, X.-B., Nakano, S., and Sugimoto, N. (2007) Consecutive GC base pairs determine the energy barrier of DNA duplex formation under molecularly crowded conditions. *Chem. Commun. 26*, 2750–2752.
26. Flory, P. J. (1961) Phase changes in proteins and polypeptides. *J. Polym. Sci. 49*, 105–128.
27. Ross, P. D., and Sturtevant, J. M. (1960) The kinetics of double helix formation from polyriboadenylic acid and polyribouridylic acid. *Proc. Natl. Acad. Sci. U.S.A. 46*, 1360–1365.

BI801821M